

# digitalSTROM<sup>®</sup>: A centralized PLC Topology for Home Automation and Energy Management

Georg Dickmann

aizo AG, Brandstr. 33, 8952 Schlieren, Switzerland

Email: georg.dickmann@aizo.com

**Abstract**—A digitalSTROM<sup>®</sup> system is based on concentrators that reside in the distribution panel, act as power-meters for the individual distribution circuits and communicate with individual nodes installed within a home over differently modulated up- and downstream channels. This paper presents the advantages of the digitalSTROM<sup>®</sup> topology, elaborates on the modulation schemes that have been optimized to lend themselves to miniaturized implementation and quantifies the level of interference caused by typical home appliances.

## I. INTRODUCTION

The European Regulators' Group for Electricity and Gas (ERGEG) and the European Union have launched an initiative to encourage the installation of smart meters in all European homes within the next decade [1]. This has driven interest towards gaining additional insight into the actual power consumption of electrical appliances compared to simply measuring the total power consumption of a home over given timeslots as enabled by today's smart meters. Once the power consumption of individual devices or subnets can be accurately monitored, the wish to gain control over selected devices within a home seems to be a natural consequence.

The goal of digitalSTROM<sup>®</sup> is the provision of an in-home infrastructure that allows both the provision of metering information from each circuit-breaker or even from individual devices as well as the control of electrical devices based on a dedicated PLC topology. An energy provider may use this infrastructure in order to optimize the load profile. The end user will gain insight into the partitioning of his personal energy consumption and thus will be able spot 'energy leaks' while taking profit from convenience functions as typically enabled by home automation systems.

## II. THE DIGITALSTROM<sup>®</sup> TOPOLOGY

In contrast to common in-home PLC systems, digitalSTROM<sup>®</sup> does not provide direct peer-to-peer communication across the in-home wiring but uses a centralized approach where all communication is relayed by entities that are installed in the distribution panel. On each digitalSTROM<sup>®</sup>-enabled sub-circuit, such an entity, called digitalSTROM<sup>®</sup> meter (dSM), is installed behind the circuit breaker and serves the dual function of communication relay and sub-circuit energy meter. A sample topology is shown in figure 1. Up to 128 communication endpoints, digitalSTROM<sup>®</sup> devices (dSD), may be connected to the home wiring behind each dSM. Up to 63 dSMs are interconnected

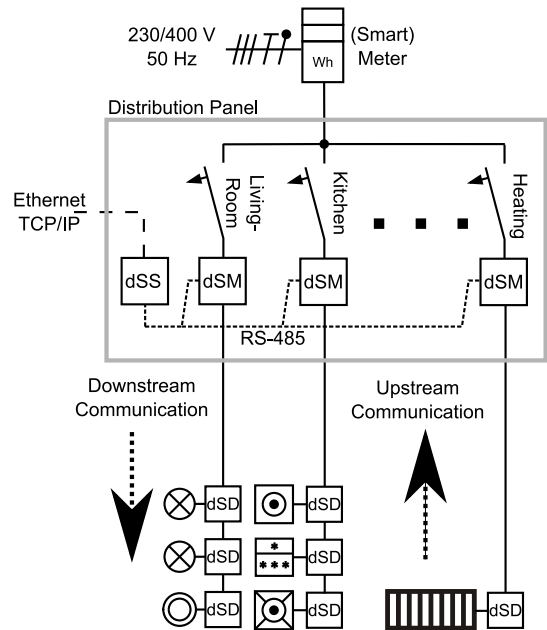


Fig. 1. Installation topology with light, washing machine, freezer, dishwasher and heating controlled by digitalSTROM<sup>®</sup> devices (dSDs).

by an RS-485 bus. The RS-485 bus further connects to a local server (dSS) through a public API [2]. The server acts as a relay to a home local area network or the internet, implements a configuration interface and allows for the implementation of tailored functions required by the end-user or the energy provider. The dSDs typically implement device-level metering functionality, are able to switch or dim the connected device and convey status information or events (e.g. "a button has been pressed") to the dSM, located upstream.

## III. THE DIGITALSTROM<sup>®</sup> PLC COMMUNICATION

The fact that dSMs are installed into the feeder cable of the in-home distribution cables offers a new degree of flexibility to the coupling of communication signals onto the mains signal since the dSM can actively manipulate the source impedance of the mains supply. Since it is able to monitor the current drawn by electrical appliances for metering purposes, it appears obvious to also use this capability for the detection of communication signals. Consequently, different signaling is used for downstream (from dSM to dSD) and upstream (from

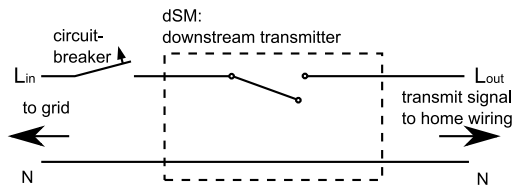


Fig. 2. Principle of downstream pulse generation.

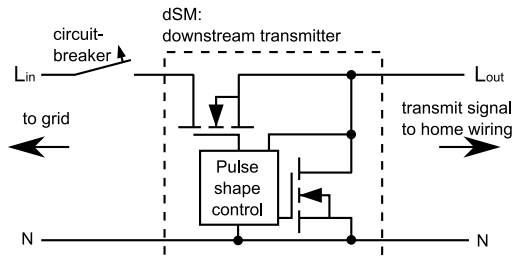


Fig. 3. Active downstream pulse shaping circuit.

dSD to dSM) communication.

#### A. Downstream Communication

1) *Physical Layer Signaling*: The downstream transmitter imposes impulses onto the mains voltage at a well-defined distance and in close proximity to the mains' zero crossings. While traditional PLC systems linearly add the transmit signal to the mains voltage, suffering from low grid impedances and thereby causing crosstalk into neighboring circuits, the approach of the downstream transmitter is to temporarily cut a distribution circuit from the supplying grid. This causes only minimum crosstalk into the grid and does not require a powerful transmitter. Figure 2 illustrates this principle by the example of a simple switch that is opened for the duration of a downstream impulse. In order to comply with the EMC-limits as imposed by [3] and [6] while keeping the pulse-shape independent from the actual load, the transmitter is implemented using power MOSFETS driven by a pulse-shaping control unit as depicted in figure 3. This approach allows for an extremely compact implementation despite the enormous transmit signal amplitude. The actual shape of a downstream impulse with raised cosine slopes is shown in figure 4. Based on these impulses, a simple on-off keying is implemented where a logic '1' corresponds to presence and a logic '0' to absence of a pulse. The begin of a message is preceded by a preamble. A (7,4)-Hamming code extended by an additional parity bit is used to detect/correct isolated errors.

This results, assuming a mains frequency of 50 Hz and at most two pulses per mains half-wave, in a maximum bit-rate of 200 bit/s or 100 bit/s when transmission is restricted to positive or negative mains half-waves only. Although these transmission rates appear extremely low, they are deemed sufficient for the purpose of the level of device control targeted by digitalSTROM<sup>®</sup>. Since this throughput does not need to be shared among an entire installation but is available within

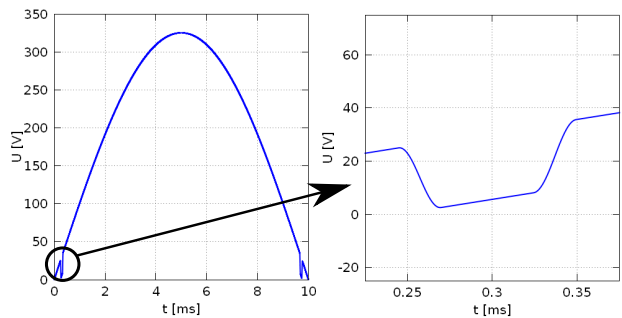


Fig. 4. Mains voltage with downstream transmission impulses. Left: Mains half-wave. Right: Enlarged pulse.

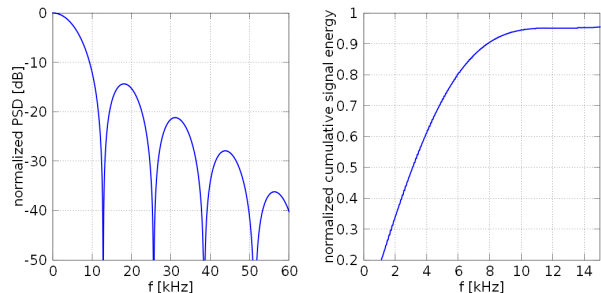


Fig. 5. Left: Normalized power spectral density of the downstream transmission pulse from Fig. 4. Right: Normalized cumulative downstream pulse energy over frequency. (60% of the pulse's energy is represented by frequency components below 4 kHz, 80% in frequency components below 6 kHz)

every mains circuit that is equipped with a dSM, the aggregate throughput scales with the number of dSMs in an installation.

2) *Robustness of the Downstream Communication*: During the transmission of the downstream impulse, the downstream transmitter can be regarded as an ideal voltage source between terminals  $L_{out}$  and  $N$  shown in figure 3, independent from the impedance of the grid. As shown in figure 5, about 90% of the downstream pulse energy is contained in the frequency range from DC to 8 kHz. The signal attenuation in this frequency range is negligible because of the short cable lengths within home installations [4] and the low source impedance of the downstream transmitter.

Potential interferers are switched electrical loads where we need to distinguish between mains-asynchronous switching and devices that are switched periodically, synchronously with the mains frequency. The former are typically represented by user-switched devices and commutated electric motors, the latter by dimmers and switched-mode power supplies. Measurements with a large number of electrical appliances have revealed that among the asynchronous disturbers, only the inrush current of large transformers and motors was causing voltage dips with amplitudes similar to those of the downstream impulses. Since these events happen only rarely and tend to have low amplitudes in close proximity to the mains zero-crossing, the error-correcting Hamming-code was found to be sufficiently strong to guarantee reliable communication.

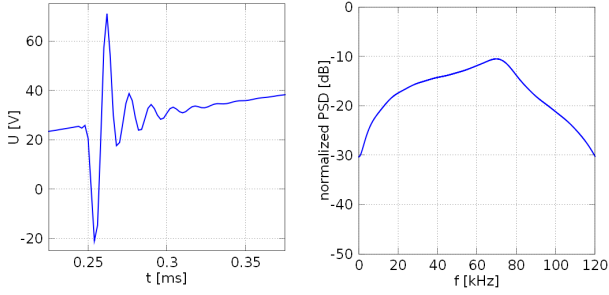


Fig. 6. Left: Impulsive disturber as caused by the inrush current of an electric drill. Right: Power spectral density of the disturber's impulse normalized to the same scale as in Fig. 5(left).

Figure 6 shows a typical asynchronous disturber caused by the inrush current of an electric drill with its associated power spectral density. Comparing this with the downstream transmission impulse clearly shows that correct downstream detection is still possible.

Among the mains-synchronous disturbers, switched-mode power supplies were found to not cause any substantial interference in close proximity to the mains zero-crossing. Similarly, conventional leading or trailing edge dimmers do not switch within a millisecond from the zero crossing.

Further interference is to be expected from ripple control systems that impose signals at frequencies from 167 to 2000 Hz onto the mains voltage using levels that typically range from 1.7 to 4% of the mains voltage [5]. Since ripple control signals (the duration of a ripple control pulse is typically greater than 150 ms) are slowly ramped up/down, there is no impulsive interference to be expected that could hide a downstream impulse.

## B. Upstream Communication

1) *Upstream topology*: In conventional PLC systems, the transmitter acts as voltage source and the received signal is detected at any point within an installation across the line terminals as shown in figure 7. In order to reduce the signal attenuation across different mains phases, phase couplers are frequently inserted between phases such that an entire installation becomes a shared medium with only limited protection against crosstalk into neighbouring installations that share the same feeder cable. Especially low-bitrate PLC systems operating within the CENELEC bands [6] suffer from low mains impedances that can reach values as low as  $0.1 \Omega$  [7], [8], [9], [10] such that substantial transmit power is required in order to obtain acceptable signal levels at the receiver.

The upstream approach of digitalSTROM<sup>®</sup> benefits from its centralized topology with a dSM behind each circuit breaker as shown in figure 8. The transmitter is implemented as current source. The dSM implements a current sensor that recovers the received signal. Consequently, the lower the grid impedance relative to the input impedance of electrical appliances within the same circuit, the higher is the signal level at the receiver. In order to keep the grid impedance low, a capacitor is inserted

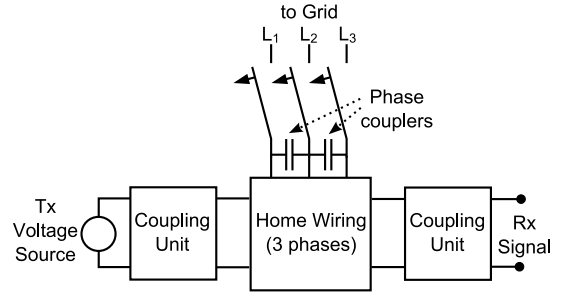


Fig. 7. Conventional in-home PLC signal coupling. A voltage signal is added to the mains signal. Propagation across phases is achieved through phase couplers.

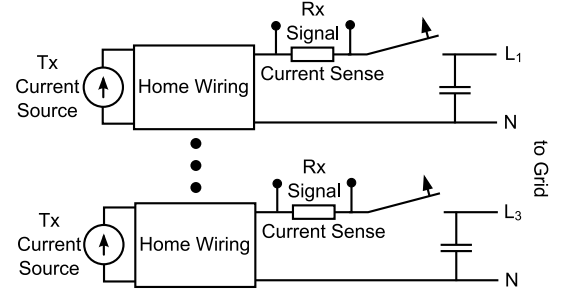


Fig. 8. digitalSTROM<sup>®</sup> upstream signal coupling. A current signal is generated by endpoints and detected by a current sensor located in the distribution panel. Capacitors between phases  $L_k$  and neutral (N) keep the source impedance low and reduce crosstalk between individual circuits.

between neutral N and each of the mains phases  $L_k$ . These capacitors serve the additional purpose of separating each circuit (each circuit-breaker / dSM defines a different circuit) into a distinct communication domain, preventing the communication signals from causing crosstalk into neighbouring installations and at the same time shielding from interference originating from the grid. Thus, the upstream channel capacity is available once per circuit in contrast to conventional systems where the available channel capacity is to be shared within an entire installation, eventually extending into neighbouring installations and/or PLC-communication deployed over the feeder cable.

2) *Upstream signaling*: The upstream modulation uses Spread-FSK where two sets of carrier frequencies are foreseen:

- A)  $T_{\text{sym},A} = 384 \mu\text{s}$ ,  $f_{\text{lower},A} = 15.625 \text{ kHz}$ ,  $f_{\text{upper},A} = 20.83 \text{ kHz}$ .
- B)  $T_{\text{sym},B} = 200 \mu\text{s}$ ,  $f_{\text{lower},B} = 100 \text{ kHz}$ ,  $f_{\text{upper},B} = 110 \text{ kHz}$ .

Carrier set A) is within the CENELEC A-Band [6] and, as such, reserved for supervision and control of the low voltage grid, explicitly including metering applications. Carrier set B) is located in the CENELEC B-Band, allowing unrestricted use by individuals.

3) *Transmitter implementation*: While conventional transmitters require a power amplifier in front of a transformer for galvanic insulation and a capacitor for separation from the mains voltage, the digitalSTROM<sup>®</sup> upstream transmitter

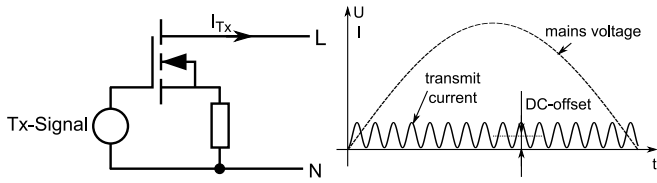


Fig. 9. Left: Transmitter implementation. Right: Transmit current DC-offset.

connects a current source as depicted in figure 9 (left) directly to the mains terminals. Here, the signal source requires only marginal power to drive the current source. Consequently, this approach allows for an extremely compact transmitter implementation. This advantage is traded against low power efficiency. Assuming that a sinusoidal signal is to be transmitted, this can be only achieved when with an associated DC-current as shown in figure 9 (right) of  $I_{DC} \geq \sqrt{2} \cdot I_{AC,RMS}$ . A transmit current of  $I_{AC,RMS} = 35 \text{ mA}$  results in a power dissipation by the transmitter of

$$P_{Tx} \geq U_{\text{mains,RMS}} \cdot \sqrt{2} \cdot I_{AC,RMS} = 230 \text{ V} \cdot \sqrt{2} \cdot 35 \text{ mA} = 11.4 \text{ W}.$$

Obviously, restricting transmission to timeslots within proximity of the mains zero-crossing will result in a reduction of the power dissipation. Similarly, using a rectangular transmit signal would reduce the power dissipation by a factor of  $\sqrt{2}$  at identical  $I_{AC,RMS}$ . However, due to EMC-constraints, this approach cannot be fully exploited.

Since digitalSTROM<sup>®</sup> endpoints are typically required to generate only a few transmission bursts per day to signal meter reading statistics or user-actions like switching of light, power efficiency of the transmitter is restrictive only in terms of instantaneous heat dissipation by the miniaturized endpoints. The duration of continued transmission has therefore been limited by appropriate design of the application protocol.

4) *Upstream channel properties:* The feeder-side capacitor (see figure 8) reduces the impact of interference originating from the feeder cable or neighboring circuits such that, in a first approach, interference from within a single distribution circuit is expected to dominate. External interference is not considered in the following.

Among electrical home-appliances, non-linear or switching devices are expected to cause the most significant levels of interference. Since, for the relevant configuration depicted in figure 8, no interference models are known, both interference levels and signal attenuation caused by about 150 different appliances have been measured using the setup shown in figure 10. The transmitter was stepping through sinewaves of different frequencies. The received signal was passed through a band-pass filter with a passband from 7 to 130 kHz. Connecting a leading-edge dimmer, driving a 500 W halogene light as electrical appliance, the recorded time domain signal (while the transmitter was silent) is shown on the left side of figure 11. The right side of figure 11 shows the signal-to-interference ratio over the position within the mains half-wave for various transmit frequencies ranging from 10 to

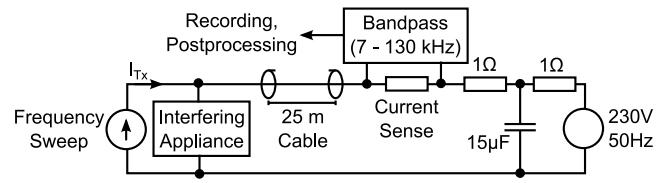


Fig. 10. Measurement setup used to assess interference levels and signal attenuation caused by electrical appliances.

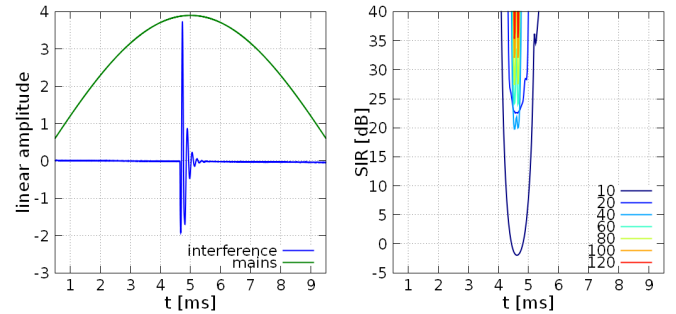


Fig. 11. Interference caused by a leading-edge dimmer dimmed to about 50%. Left: time-domain view of a single mains half-wave. Right: signal-to-interference ratio over time within a mains half-wave for frequencies ranging from 10 to 120 kHz relative to a transmit current of  $I_{Tx,RMS} = 35 \text{ mA}$ .

120 kHz relative to a transmit current of  $I_{Tx,RMS} = 35 \text{ mA}$ . Most devices were found to cause a stationary interference pattern repeating itself at twice the mains frequency. Signal-to-interference ratios measured with other electrical appliances that were found to cause significant levels of interference are shown in figure 12.

The measured signal-to-interference ratios show that the interference levels generally decrease with increasing frequency. The lower the frequency, the more the interference levels were found to fluctuate over a mains half-period. Generally, the interference levels were observed to be lowest in close proximity of the mains zero-crossings.

With the given transmit current of  $I_{Tx,RMS} = 35 \text{ mA}$ , the signal-to-interference ratios were, except from the carrier frequency at 10 kHz, generally far better than 3 dB allowing for reliable detection of an FSK-encoded signal. Note that the observed signal-to-interference levels cannot be mapped to error probabilities since the interference characteristics does not match those of an AWGN (additive white Gaussian) channel. The interference was typically caused by a single or very few repetitive sources and, as such, will not exhibit a Gaussian distribution.

a) *Worst-case considerations:* While the results shown in figure 12 exhibit all very comfortable signal-to-interference ratios, those will be degraded in scenarios like the one depicted in figure 13. In the frequency range of interest ( $10 \text{ kHz} < f < 150 \text{ kHz}$ ), a typical in-house installation cable with a cross-section of  $1.5 \text{ mm}^2$  can be modeled as inductance with  $L'_{\text{cable}} \approx 0.4 \frac{\mu\text{H}}{\text{m}}$ . In typical installations conforming to [4], the maximum length of an installation with the given cross-

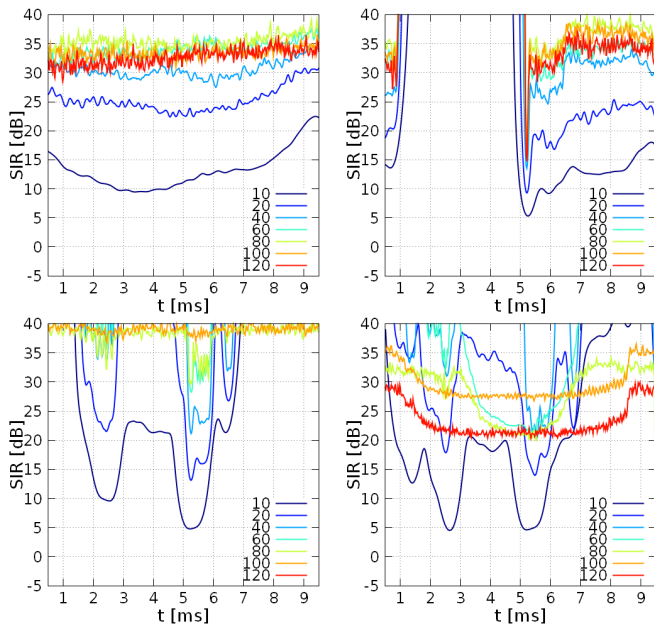


Fig. 12. Signal-to-interference ratios over time within a mains half-wave for frequencies ranging from 10 to 120 kHz relative to a transmit current of  $I_{Tx,RMS} = 35$  mA. Upper left: An electric drill. Upper right: A vacuum cleaner operated at reduced power. The 'dimming' is implemented by a leading-edge dimmer as can be seen from the low interference levels in the first half of the mains half-period. Lower left: A modern TV-set with a 210 Watt switched mode power supply. Lower right: the same TV-set as on the left but with 4 additional switched-mode laptop power supplies.

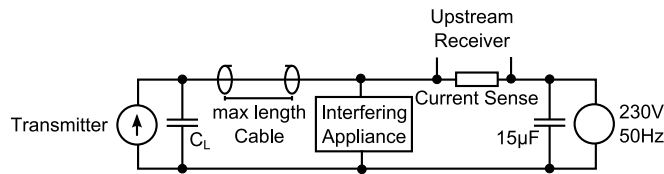


Fig. 13. Worst-case upstream communication scenario where the upstream transmitter is located at the far end of a long installation cable, an interferer is next to the receiver and a capacitive load  $C_L$  is placed next to the transmitter.

section is expected to never exceed 50 m, corresponding to a cable inductance of  $L_{cable} = 20 \mu\text{H}$ . The maximum value of a capacitive load  $C_L$  is, however, not bounded. Many modern appliances have an anti-interference capacitor across their supply terminals. Among a tested set of 150 electronic devices, input-terminal capacities of up to  $1 \mu\text{F}$  have been measured. Assuming a maximum capacity of  $4 \mu\text{F}$ , the worst-case scenario from figure 13 translates into the simplified worst-case attenuation model shown in figure 14. Assuming that the measured signal-to-interference levels displayed in figure 12 can be translated into worst-case levels by adding the gain from figure 14 (Right) the resulting signal-to-interference levels will be just sufficient for the correct decoding of the received signal.

*b) Measurements results from a worst-case installation:*

Figure 15 shows measurements from a home installation in a configuration that is considered to represent a difficult

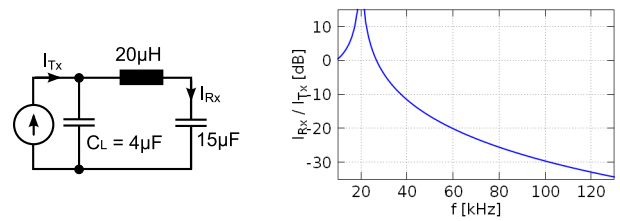


Fig. 14. Left: Simplified upstream worst-case attenuation scenario. Right: Resulting channel gain over frequency.

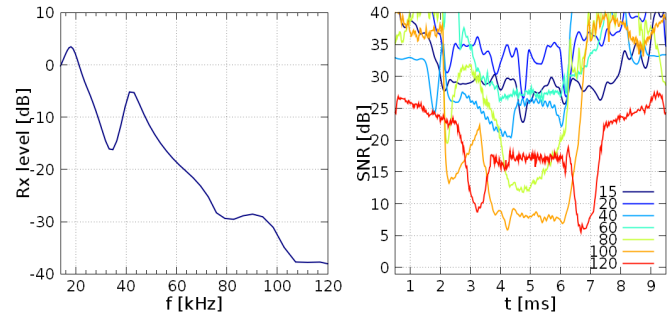


Fig. 15. Left: Signal attenuation over frequency. Right: Signal-to-interference ratios over time within a mains half-wave for frequencies ranging from 15 to 120 kHz relative to a transmit current of  $I_{Tx,RMS} = 35$  mA.

environment:

The upstream transmitter was placed at maximum distance to the receiver ( $\approx 20$  m). Various active electrical appliances were being connected at different places to the same electrical circuit:

- A 40 inch LCD-TV.
- 7 metal halide lamps (20 – 35W each).
- 2 PCs.
- A 7x180 W audio video receiver.
- A 300 W HiFi subwoofer.
- 20 W LV halogene lamp with electronic transformer.
- Various small electronic devices (WLAN-router, cable-modem, settop box, DECT-telephone, SIP-gateway)

Under these conditions, the upstream communication based on the carrier set in the CENELEC A-band was found to operate without any communication errors.

5) *Upstream channel code:* The channel code needs to counter impulsive noise while the level of interference varies with the mains phase and is periodic with twice the mains frequency. Therefore, a convolutional code in conjunction with an interleaver was selected. The interleaver depth was chosen to equal the number of channel bits transmitted within a mains half-period in order to keep the length of error events well below the constraint-length of the convolutional code. The

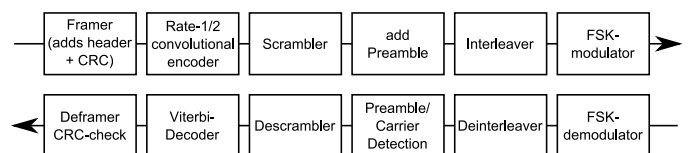


Fig. 16. Upstream encoding/decoding chain.

complete encoding/decoding-chain is sketched in figure 16.

#### IV. COEXISTENCE WITH OTHER PLC-TECHNOLOGIES

##### A. PRIME

The PRIME alliance has drafted a PLC-system for operation in the CENELEC A-band for the purpose of meter-reading [11]. The carriers of the underlying OFDM modulation occupy the frequency range from 41 – 89 kHz and, as such, do not overlap with the digitalSTROM<sup>®</sup> system. However, the capacitors that are typically inserted on each of the mains phases in the distribution panel of a digitalSTROM<sup>®</sup> installation will reduce the mains impedance in the vicinity of the power meter leading to additional attenuation of the PRIME's signal.

##### B. G3

Similar to the PRIME specification, the base G3 specification [12] foresees operation in the CENELEC A band in a frequency range from 36 – 90 kHz. Consequently, the frequencies do not overlap with those of the digitalSTROM<sup>®</sup> system but, again, due the capacitors inserted by digitalSTROM<sup>®</sup> into the distribution panel, the G3 signal is likely to incur some extra attenuation. It is expected that devices built according to the G3 extension for operation in the CENELEC B-band will not be able to coexist with a digitalSTROM<sup>®</sup> installation.

##### C. IEEE 1901.2

The P1901.2 project targets narrowband powerline communication at carrier frequencies below 500 kHz for smart grid applications through all stages (high voltage to low voltage) of the distribution network. Currently, there are not enough details available to assess potential coexistence issues.

#### V. CONCLUSION

The digitalSTROM<sup>®</sup> system has been presented as a new approach to bridge the gap between smart metering and home automation.

Its particular, centralized topology allows a new approach to PLC over in-home wiring. Tailored up- and downstream signal coupling and modulation have been presented along with an approach to implement the respective schemes. Typical interferers in the upstream communication path have been measured and a worst-case interference estimation has been attempted. The system was found to allow for reliable communication despite the low-complexity up- and downstream transmitter implementations that permit a hardware-realization in small form factors. No major coexistence hurdles with common PLC technologies were found.

#### REFERENCES

- [1] European Regulators' Group for Electricity and Gas, Smart Metering with a Focus on Electricity Regulation, Document E07-RMF-04-03, 31 October 2007.
- [2] Developer site of digitalSTROM.org at <http://developer.digitalstrom.org>.
- [3] EN 55015, Limits and method of measurement of radio disturbance characteristics of electrical lighting and similar equipment.
- [4] IEC 60364-5-52, Low-voltage electrical installations - Part 5-52: Selection and erection of electrical equipment - Wiring systems.
- [5] Rundsteuertechnik at <http://www.rundsteuerung.de>.
- [6] EN 50065-1 final draft 2010, Signalling on low-voltage electrical installations in the frequency range 3 kHz to 148.5 kHz – Part 1: General requirements, frequency bands and electromagnetic disturbances.
- [7] Arzberger, M., Waldeck, T., Zimmermann, M. and Dostert, K.: Fundamental Properties of the Low Voltage Power Distribution Grid. Proceedings of the 1997 International Symposium on Power Line Communications and its Applications (ISPLC'97), Essen, Germany, April 1997, pp. 45-50.
- [8] Arzberger, M.: Datenkommunikation auf elektrischen Verteilnetzen für erweiterte Energiedienstleistungen. Logos-Verlag Berlin, Germany, 1999
- [9] Kistner, T.: Ein neuartiges mehrträgerbasiertes PLC-System mit störresistenter Synchronisation. Doctoral Dissertation, Universitätsverlag Karlsruhe (2008) ISBN 978-3-86644-224-5
- [10] Bausch, J.: Elektrische Installationsnetze als Datenübertragungsmedium zur Gebäudeautomatisierung. Mensch&Buch-Verlag, Berlin, 2005.
- [11] Draft standard for PowerLine Intelligent Metering Evolution R1.3E, PRIME alliance.
- [12] PLC G3 physical layer specification, ÉLECTRICITÉ RÉSEAU DISTRIBUTION FRANCE (ERDF)